STEREO EVALUATION OF CARTOSAT-1 DATA FOR FRENCH AND CATALONIAN TEST SITES

Manfred Lehner, Rupert Müller, Peter Reinartz, Manfred Schroeder

German Aerospace Center (DLR), Remote Sensing Technology Institute, D-82234 Wessling, Germany

CARTOSAT-1 Scientific Assessment Program – Commission IV/WG 9

ABSTRACT:

DLR's Remote Sensing Technology Institute has more than 20 years of experience in developing spaceborne stereo scanners (MEOSS, MOMS) and the corresponding stereo evaluation software systems. It takes part in the CARTOSAT-1 Scientific Assessment Program (C-SAP) as a principal investigator for a Catalonian test site (TS-10) and as Co-Investigator for a French test site (TS-5, Mausanne-les-Alpilles).

Rational polynomial coefficients (RPC) are provided by the distributing Indian agency as a universal sensor model for each scene of the CARTOSAT-1 stereo pairs. These RPC have to be corrected via ground control points (GCP) as they are derived from orbit and attitude information with an accuracy far worse than the pixel size of 2.5 m (normally, post facto pointing accuracy is in the range of a few hundred meters). GCP of sufficient (sub-pixel) accuracy are derived from high-resolution orthoimages of the Catalonian Survey Institute (ICC) and from JRC DGPS campaigns, respectively. The GCP are identified in the aft images of the stereo pairs because of their superior radiometric quality and then transferred to the fore images via local least squares matching. From these GCP an affine correction to the delivered RPC is estimated. The residual vectors at the GCP are reduced to sub-pixel values. Because of zero denominator problems with the original RPC in small regions of the stereo pairs new RPC are estimated

Using the corrected RPC and mass tie points from automatic image matching the digital surface models (DSM) are derived from the CARTOSAT-1 stereo pairs via forward intersection and subsequent interpolation. These DSM are compared to the available sufficiently accurate DEM/DSM provided by ICC and JRC. For the comparison a 3D shift between the individual DSM is estimated via least squares adjustment. Height accuracies (in terms of 1 σ) of 2.5-4 m are achieved. The shifts between the orthoimages of the two looking directions computed on the basis of the reference DEM and the computed DSM are assessed via image matching and are found to be in sub-pixel range.

1. INTRODUCTION

1.1 General DLR stereo scanner background

DLR is engaged in 3-line stereo scanner development and data evaluation since 1980 when ISRO offered to fly such a DLR camera on SROSS-I satellite to be launched by Indian ASLV rocket in 1988. The camera has been built and the German photogrammetric community and also ISRO/SAC could exploit airborne 3-line scanner imagery of a MEOSS camera model from 1986 onwards (Lehner&Gill 1992, Heipke et al., 1996). DLR in subsequent years concentrated on the German 3-line scanner MOMS-02 which was successfully flown as MOMS-02/D2 instrument on space shuttle mission D2 in 1993 and as MOMS-2P on the Russian space station Mir from 1996 till 1999. MOMS mission brought the development of a MOMS stereo work station at DLR through cooperation of DLR with several German universities (Seige et al, 1998, Kornus et al., 2000).

As in spite of many negotiations a follow-on project (MOMS-03) did not come true DLR applied its evaluation experience to upcoming foreign missions. The next along-track stereo scanner in space was the HRS instrument on SPOT-5 (launched in May 2002). DLR took part as a PI in the HRS scientific assessment program 2003-4 (Reinartz et al, 2006).

1.2 Rigorous and replacement models in stereo evaluation

Up to SPOT-5 HRS the concept of rigorous modelling of the stereo imaging was the basis of the stereo evaluation software at DLR. Afterwards also replacement models like rational polynomial camera models (RPC) had to be considered in the advent of the commercial high resolution optical sensors IKONOS-2 and QuickBird. For these sensors special additions to the stereo evaluation software system at DLR have been made (Lehner et al, 2005/2006) along the lines given in various papers (e.g. Grodecki et al, 2004). This was a good preparation for the CARTOSAT-1 Scientific Assessment Program (C-SAP) because only replacement models have been delivered to the investigators for the CARTOSAT-1 stereo pairs up to now.

DLR is working on test site 5 (Mausanne-les-Alpilles, Southern France; PI from JRC in Ispra) and its own PI test site 10 (Catalonia). As many results from test site 5 are reported already in (Lehner et al., 2006) this paper concentrates on Catalonia.

1.3 Investigations presented in this paper

Investigations are based on delivered image data and RPC. The automatic image matching is performed with DLR software to give mass tie points.

A new aspect besides new data on Catalonia is the detection of RPC zero denominator problems which had not yet been treated in (Lehner et al., 2006). In the course of these investigations tests for the generation of new RPC from the old ones, already including the affine transformation correction based on ground control points, have been performed. By reducing the number of coefficients of the RPC the zero denominator problem could be avoided. It turned out that 49 (keeping only the quadratic terms

and using one common denominator polygon for rows and columns) coefficients are sufficient to achieve the same accuracy in elevation modelling and orthoimage generation.

The summary of first results presented in (Lehner et al., 2006) which in essence are consolidated by the investigations of this paper is:

- The RPC delivered together with CARTOSAT-1 stereo pairs have to be corrected via an affine transformation based on (at least 3) ground control points of sufficient (i.e. sub-pixel) accuracy well distributed over the images.

- After this correction is done a DSM accuracy of 2.5-4 m (1 σ) can be achieved. The shifts between orthoimages of aft and fore sensors produced with this DSM are in the order of fractions of pixels in all parts where DSM modelling succeeded (enough tie points via automatic matching).

2. CARTOSAT-1 DATA AND GROUND TRUTH

2.1 Test site 5 – Mausanne-les-Alpilles

2 CARTOSAT-1 stereo pairs (see MA/F1 and MA/F2 of table 2-1) are provided. DEM and ground control points (GCP) are provided by JRC.

Table 2-1: CARTOSAT-1 stereo pairs used (GCP: - means no GCP or not sufficiently accurate)

Stereo pair (aft, fore)		Acquisition date	Region	GCP
MA1	MF1	31Jan06	Mausanne	30
MA2	MF2	06Feb06	Mausanne	-
CatA	CatF	01Feb06	Catalonia	70
SfrA	SfrF	20Jul06	Hautes Alpes	-

A reference DEM of most of the area of the test site 5 and ground control point coordinates measured by GPS survey and corresponding image chips and photos of the measurement configurations have been delivered by the PI of test site 5 from JRC. In (Lehner et al., 2006) 13 GCP were measured at DLR. These are replaced here by the 30 GCP measured by JRC.

2.2 Test site 10 - Catalonia

A stereo pair is provided. A reference DEM and orthoimages with scale 1:5000 are provided by ICC. 70 GCP have been measured in the orthoimages and the stereo partner CatA with sub-pixel precision. These measurements have been automatically transformed into CatA/F tie points via least squares matching using mass points from hierarchical matching (see next section) for initial guesses of CatF coordinates and least squares matching (LSM) with several window sizes. Thus, 68 GCP for CatF could be derived – well fitting to the CatA GCP in terms of stereo tie points. 6 window sizes from 17 to 27 have been used in LSM in order to get statistical values for the accuracy. The mean standard deviations in rows and columns for the 68 GCP and 6 window sizes were below 0.1 pixel.

2.3 Matching for tie point generation

Hierarchical intensity based matching as implemented into the XDibias image processing system of DLR consists of two major steps.
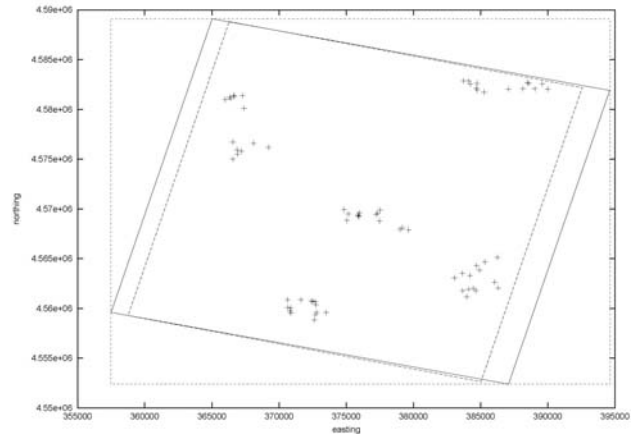

Figure 2-1: CARTOSAT stereo pair, ICC reference DEM and distribution of GCP extracted from the 10 orthoimages of scale 1:5000 (GCP: +, reference DEM: small dashes, CatA: larger dashes, CatF: full line)

In a first step the matching process uses a resolution pyramid (Lehner&Gill, 1992; Kornus et al., 2000) to cope even with large stereo image distortions stemming from carrier movement and terrain. Large local parallaxes can be handled without knowledge of exterior orientation (which is often not available with sufficient accuracy – much improvements have been made in this respect in the near past, though). The selection of pattern windows is based on the Foerstner interest operator which is applied to one of the stereo partners. For selection of search areas in the other stereo partner(s) local affine transformations are estimated based on already available tie points in the neighborhood (normally from a coarser level of the image pyramid). Tie points with an accuracy of one pixel are located via the maximum of the normalized correlation coefficients computed by sliding the pattern area all over the search area. These approximate tie point coordinates are refined to sub-pixel accuracy by local least squares matching (LSM). The number of points found and their final (sub-pixel) accuracy achieved depend mainly on image similarity and decrease with increasing stereo angles or time gaps between imaging. The software was originally devised for along-track 3-line stereo imaging (stereo scanners MEOSS and MOMS operated by DLR). Normally, the procedure can be executed fully automatically if the shift between the stereo partners is small compared to the image size as is true for CARTOSAT-1 stereo pairs. The procedure results in a rather sparse set of tie points well suited for introducing them into bundle adjustment and as an excellent source of seed points for further densification via region growing (second step).

The second step uses the region growing concept first published by Otto and Chau in the implementation of TU Munich (Heipke et al., 1996). It combines LSM with a strategy for local propagation of initial conditions of LSM.

Various methods for blunder reduction are used for both steps of the matching:

- Threshold for correlation coefficient
- 2-directional matching and threshold on resulting shifts of the coordinates
- Threshold on residuals (in image space) from forward intersection based on the rigorous modeling of the imaging process or on rational polynomial functions (RPC).

In areas of low contrast the propagation of affine transformation parameters for LSM in the region growing process leads to high

rates of blunders. In order to avoid intrusion into homogeneous image areas (e.g. roof planes without structure) the extracted image chips are subject to (low) thresholds on variance and roundness of the Foerstner interest operator. This and the many occlusions found in densely built-up areas imaged with a large stereo angle create lots of insurmountable barriers for region growing. Thus, for high resolution stereo imagery the massive number of seed points provided by the matching in step one (image pyramid) turns out to be essential for the success of the region growing.

The numbers of tie points found and their sub-pixel accuracy is highly dependent on the stereo angle. A large stereo angle (large base to height ratio b/h) leads to poorer numbers of tie points and to lower accuracy in LSM via increasing dissimilarity of (correctly) extracted image chips.

3. RPC USAGE WITHOUT CORRECTION

For IKONOS and QuickBird stereo pairs RPC are relatively corrected using residuals of forward intersection for (carefully selected) tie points from matching to give a system of RPC for the generation of fitting triples of orthoimages and DSM. Normally, IKONOS-2 stereo pairs are already delivered with zero mean residuals via relative bundle adjustment during RPC generation. The absolute positional accuracy of this type of imagery (IKONOS: below 10 m, see Ager, 2003 and Eisenbeiss et al., 2004) is already very high and forward intersection is giving high percentages of accepted points with relatively strict thresholds (for this paper: 0.5 pixel) on residuals in image space.

The absolute positional accuracy of CARTOSAT-1 images is in the order of a few hundred meters only. Thus, the modelling of the imaging conditions is weak. Normally, with uncorrected RPC high rates of non accepted points result from forward intersection. Thus, relative correction of RPC in case of CARTOSAT-1 does not lead necessarily to nice relative stereo models and orthoimages (MA/F1 seems to be an exception). After absolute correction with GCP the conditions for forward intersection are much improved for stereo pair CatA/F as is shown in table 3-1. The situation is of course quite similar to insufficient ground truth in rigorous modelling.

Table 3-1: Percentage of accepted points in forward intersection before and after use of accurate GCP

Stereo pair	Tie points	Percentage acc. points	Accurate GCP	Percentage acc. points
MA/F1	8498	99.1	30	99.1
MA/F2	25574	33.9	-	-
CatA/F	58856	45.6	70/68	99.9
SfrA/F	11698	36.0	-	-

CARTOSAT-1 RPC delivered for MA/F1 and CatA/F (and other stereo pairs) show zero denominator problems in some small areas of the images. This leads to artefacts in orthoimages and DSM (see generation of new RPC below).

4. RPC ABSOLUTE CORRECTION

4.1 RPC correction via affine transformation

Thus, correction via full affine transformation is necessary as already documented in (Lehner et al., 2006). The correction equations are as follows:

$$row = a_0 + a_1 RPC_{row} + a_2 RPC_{col}$$
$$col = b_0 + b_1 RPC_{row} + b_2 RPC_{col}$$
$$where \quad RPC_{row} \, and \, RPC_{col} \quad are \, the \, originally$$
$$provided \, rational \, polynomial \, functions$$

In case of Catalonia the estimation of affine transformation is based upon the 70/68 GCP for each of the two stereo partners. The standard deviations of the residuals are given in table 4-1 and drop below 1 pixel. Table 4-1 also gives the shift parts of the affine transformations as an indication of the absolute positional accuracy of the original RPC.

Table 4-1: shift parts of affine transformations and standard deviations of residuals (in pixel) for affine correction of RPC (6 coarse GCP in case MA/F2)

image	number of GCP	shift part of aff.tr.		σ of residuals	
		row	column	row	column
MA1	31	-2257.4	-786.2	0.76	0.56
MF1		-2154.3	-640.2	0.71	0.68
MA2	6	-71.0	-10.7	1.50	1.28
MF2		130.1	-11.0	1.35	0.81
CatA	70	-62.2	-27.5	0.51	0.41
CatF	68	134.0	-11.5	0.56	0.44

Figures 4-1 and 4-2 show the residuals in image space at the locations of the GCP for aft and fore sensors, respectively. No systematic effects show up. The standard deviations of the residuals can not drop to lower values because the identification accuracy of the GCP can not be brought down substantially below one half pixel (at least for not especially signalized targets).
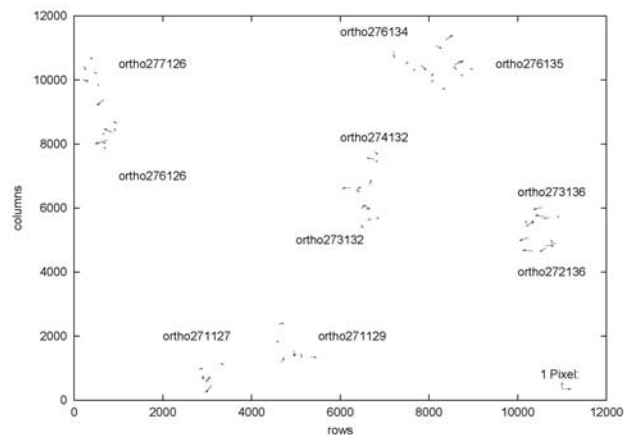

Figure 4-1: Deviations in pixel (factor 200 enlarged) of measured versus RPC image coordinates after affine transformation correction of RPC at 70 GCP (CatA – orthoimage names in row/col nomenclature of ICC)
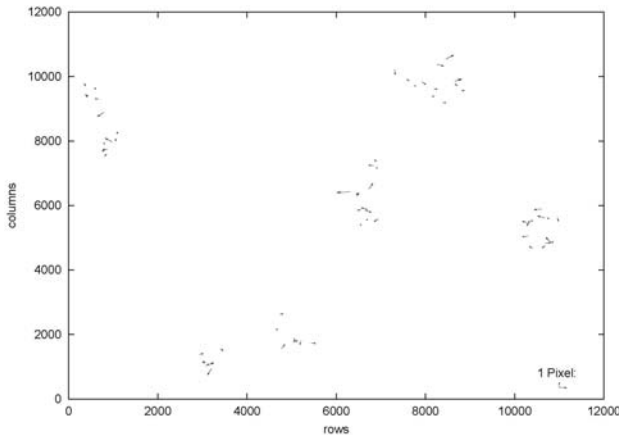
Figure 4-2: Deviations in pixel (factor 162 enlarged) of measured versus RPC image coordinates after affine transformation correction of RPC at 68 GCP (CatF)

5. GENERATION OF NEW RPC

Because of the zero denominator problems with the provided RPC new RPC have been generated for the CARTOSAT-1 stereo pairs. It was found that like IKONOS-RPC there can be a common denominator polynomial for row and column RPC. Furthermore, it is sufficient to take the linear and quadratic terms. Thus, the total number of coefficients for a stereo pair is reduced to 49 in contrast to 158. These new RPC are free of the zero denominator problem.

For each point of an artificial 3D-grid on latitude, longitude and ellipsoidal height in WGS84 datum the correspondence of the (line, column)-coordinates and (latitude, longitude, height)-triple is calculated using the affine corrected (original) RPC. Via least squares adjustment the new RPC coefficients are calculated. The standard deviations of the residuals at about 4000 artificial GCP are given in table 5-1. These standard deviations can be tolerated when compared to the standard deviations left after affine transformation shown in table 4-1. Some hints for the generation of RPC were taken from (Grodecki&Dial, 2001, and Hye-jin Kim et al, 2002).

Table 5-1: Residuals in image space from adjustment of new RPC via original RPC and affine transformation correction for Catalonia

image	Nr. 3D-GCP	σ-row	σ-column
CatA	4083	0.03	0.01
CatF	4002	0.12	0.11

6. COMPARISONS

In order to compare the reference DEM of ICC with the newly generated DSM from the Catalonian stereo pair 3D shifts are calculated between the reference DEM and the point clouds generated via forward intersection. The analysis is based on an iterative least squares adjustment with the height differences as observations. Two calculations are presented here:

- Point cloud 1 comprising points over the full area of the stereo pair derived via region growing with a step size 3 (to cope with the vast amount of data)

- Point cloud 2 with points from the left upper quarter scene which is much more dense with a step size 1 in region growing

The results are given in table 6-1. The good height accuracy of about 2.5 m (1 σ) over all classes of land use is very satisfactory. The negative Δz means that the DSM is slightly above the DEM what is to be expected. The higher value of Δy in case of the upper left quarter can indicate a small rotation of the DEM and DSM versus each other, which is not estimated by the adjustment. Large forested areas are found in the upper left quarter. This can explain the larger absolute value of Δz and shows up also in the full orthoimage comparison based on the calculation of the orthoimages with the reference DEM.

Table 6-1: Estimated 3D shifts between reference DEM and DSM point clouds for Catalonia

CatA/F	Number of DSM points	3D shift			σz
		Δx	Δy	Δz	
Full scene	6.79 million	0.4	-1.1	-0.5	2.4
UL quarter	16.49 million	0.6	-3.4	-1.7	2.6

Interpolation of the point clouds was done with DLR software described in (Hoja et al, 2005). The resulting DSM from the upper left quarter scene was used to compute orthoimages of aft and fore sensor based on the new RPC. The shifts between these images are assessed via image matching. The individual shifts are averaged over cells of about 100 x 100 pixels and shown in figure 6-1. The pixel size of the orthoimages is 2.5 m. The low values of means and standard deviations for row and column shifts are indicated.
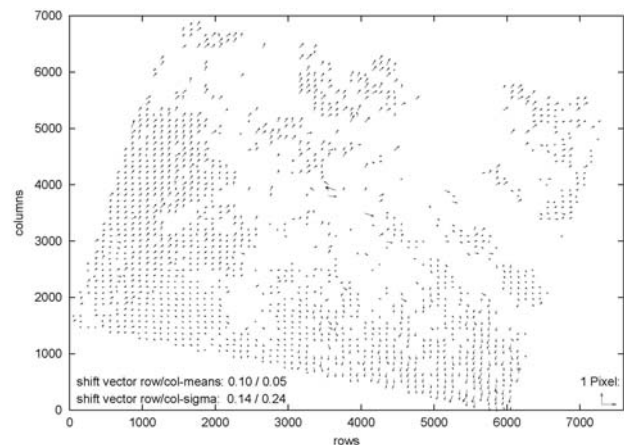

Figure 6-1: Shifts (in pixel / factor 200 enlarged) derived via automatic image matching between the Aft/Fore orthoimages generated with new RPC and DSM derived from CARTOSAT-1 stereo pair (upper left part)

For the shift patterns in figure 6-2 the reference DEM was taken as the basis for the calculation of orthoimages of the full stereo partners (same new RPC). One can easily see that the reference DEM is less suited for this calculation because many 3D objects like trees and houses are not represented. Whereas the overall mean shift is of the same order, especially in the more densely forested region of the upper left part the shifts caused by the tree height can be recognized well.
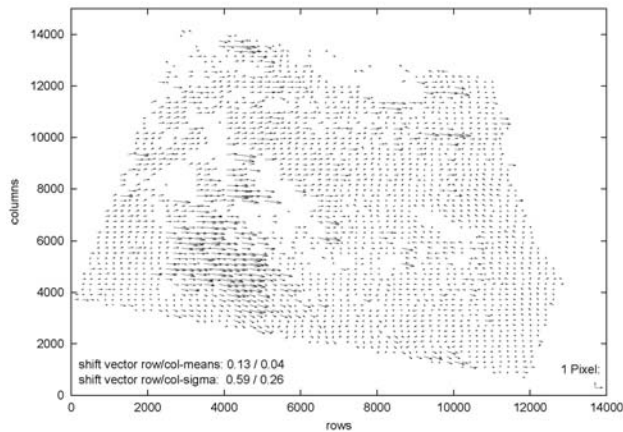
Figure 6-2: Shifts (in pixel / factor 200 enlarged) between the Aft/Fore orthoimages generated with new RPC but reference DEM (full stereo scene)

7. CONCLUSIONS

CARTOSAT-1 stereo pair on Catalonia is thoroughly studied. Most results reported in (Lehner et al., 2006) could be confirmed, especially that RPC can and have to be corrected via an affine transformation computed with well distributed and sufficiently accurate ground control points.

The large residuals in the order of kilometres which had been found for stereo pair MA/F1 are now classified as an exceptional case. Normally, residuals of a few hundred meters are to be expected. Comparisons of the generated DSM with the JRC and ICC reference DEM via estimation of 3D shifts result in standard deviations of the height differences of 2.5-4 meters for affine correction of RPC. This should be ranked as a very good result because no object classification in terms of DSM/DEM differences is applied. Thus, CARTOSAT-1 stereo imagery is well suited for the derivation of DSM and orthoimages with about one half pixel lateral and 1-2 pixel vertical accuracy (1 σ) in terrain with good pattern matching characteristics and moderate slope angles.

References from Journals:

Heipke, C., Kornus, W., Pfannenstein, A., 1996. The evaluation of MEOSS airborne 3-line scanner imagery – processing chain and results, Photogrammetric Engineering and Remote Sensing, Vol. 62, No. 3, pp. 293-299

Kornus W., Lehner M., Schroeder, M., 2000, Geometric inflight calibration by block adjustment using MOMS-2P 3-line-imagery of three intersecting stereo-strips, SFPT (Société Francaise de Photogrammétrie et Télédétection) , Bulletin Nr. 159, pp. 42-54

Reinartz, P., Müller, Rupert, Lehner, M., Schroeder, M., 2006: Accuracy Analysis for DSM and orthoimages derived from SPOT HRS stereo data using direct georeferencing, ISPRS Journal of Photogrammetry & Remote Sensing 60, pp. 160-169

References from Other Literature:

Ager, T. P., 2003: Evaluation of geometric accuracy of Ikonos imagery, SPIE 2003 AeroSense Conference, Orlando, Florida, USA

Eisenbeiss, H., Baltsavias, E., Pateraki, M., Zhang, L., 2004. Potential of Ikonos and Quickbird imagery for accurate 3D point positioning, orthoimage and DSM generation. International Archives of Photogrammetry, Vol 35, Part B, 20th ISPRS Congress, Istanbul

Grodecki, J., Dial, G., 2001 : IKONOS Geometric Accuracy, Proceedings of Workshop on High Resolution Mapping from Space, Sept. 19-21, Hannover, Germany

Grodecki, J., Dial, G., Lutes, J., 2004. Mathematical Model for 3D feature extraction from multiple satellite images described by RPCs. ASPRS Annual Conference Proceedings, Denver, Colorado, USA

Hoja, D., Reinartz, P., Lehner, M., 2005: DSM Generation from High Resolution Satellite Imagery Using Additional Information Contained in Existing DSM. Proceedings of the ISPRS Hannover Workshop 2005 High Resolution Imaging for Geospatial Information, Hannover, Germany

Hye-jin Kim, Dae-sung Kim, Hyo-sung Lee, Yong-il Kim, 2002: A Study on the Generation of the KOMPSAT-1 RPC Model, ISPRS Commission III Symposium, Sept. 9-13, Graz, Austria

Lehner M., Gill, R.S., 1992: Semi-Automatic Derivation of Digital Elevation Models from Stereoscopic 3-Line Scanner Data, *IAPRS,* Vol. 29, part B4, Commission IV, pp. 68-75, Washington, USA

Lehner, M., Müller, Rupert, Reinartz, P., 2005: DSM and Orthoimages from QuickBird and Ikonos Data Using Rational Polynomial Functions, Proceedings of "High Resolution Earth Imaging for Geospatial Information", May 17-20, Hannover, Germany

Lehner, M., Müller, Rupert, Reinartz, P., 2006: Stereo Evaluation of CARTOSAT-1 Data on Test Site 5 – First DLR Results, Proceedings of ISPRS-TC IV Symposium, Sept. 27-30, Goa, India

Seige, P., Reinartz, P., Schroeder, M., 1998: The MOMS-2P mission on the MIR station, *IAPRS,* Vol. 32, Part 1, pp. 204-210, Bangalore, India (see also http://www.nz.dlr.de/moms2p)